Fiber optical parametric oscillator for coherent anti-Stokes Raman scattering microscopy

Erin S. Lamb,[1,*] Simon Lefrancois,[1] Minbiao Ji,[2] William J. Wadsworth,[3] X. Sunney Xie,[2] and Frank W. Wise[1]

[1]*School of Applied and Engineering Physics, Cornell University, Ithaca, New York 14853, USA*

[2]*Department of Chemistry and Chemical Biology, Harvard University, Cambridge, Massachusetts 02138, USA*

[3]*Centre for Photonics and Photonic Materials, University of Bath, Bath, BA2 7AY, UK*

*Corresponding author: ecs223@cornell.edu

We present a synchronously pumped fiber optical parametric oscillator for coherent anti-Stokes Raman scattering microscopy. Pulses from a 1 μm Yb-doped fiber laser are amplified and frequency converted to 779–808 nm through normal dispersion four-wave mixing in a photonic crystal fiber. The idler frequency is resonant in the oscillator cavity, and we find that bandpass filtering the feedback is essential for stable, narrow-bandwidth output. Experimental results agree quite well with numerical simulations of the device. Transform-limited 2 ps pulses with energy up to 4 nJ can be generated at the signal wavelength. The average power is 180 mW, and the relative-intensity noise is much lower than that of a similar parametric amplifier. High-quality coherent Raman images of mouse tissues recorded with this source are presented.   © 2013 Optical Society of America

OCIS codes: (180.5655) Raman microscopy; (190.4970) Parametric oscillators and amplifiers; (320.7140) Ultrafast processes in fibers.

http://dx.doi.org/10.1364/OL.38.004154

Coherent anti-Stokes Raman scattering (CARS) microscopy offers label-free, three-dimensional optical sectioning of biological tissue by utilizing intrinsic molecular vibrations [1]. The source needed for this technique must supply two narrow-bandwidth, synchronized picosecond pulse trains with a frequency difference tunable to the relevant Raman shift. Transform limited, few-picosecond pulses are ideal for achieving the highest peak power while filling the Raman vibrational lineshape. The majority of CARS imaging experiments are conducted using a frequency-doubled Nd-YVO$_4$ laser to synchronously pump a bulk optical parametric oscillator (OPO) [2]. The complexity and large footprint of such a source hinders the widespread use of CARS microscopy.

Sources that exploit the compact and alignment-free nature of fiber could make CARS more accessible. Fiber-based sources include a frequency-doubled fiber laser used to pump a bulk OPO [3] and a two-color source based on frequency-shifting a picosecond Er-doped fiber laser to perform second-harmonic generation (SHG) [4]. Another uses the output from an Er-doped fiber laser to generate the two colors through SHG and filtering a supercontinuum generated from highly nonlinear fiber [5]. However, this source operates at low average power.

Other fiber-based sources use parametric generation. An optical parametric amplifier (OPA) was used to provide femtosecond and picosecond pulses for coherent Raman microscopy [6], but its output is too low for video-rate imaging. Other OPAs use normal dispersion four-wave mixing (FWM) in photonic crystal fiber (PCF) to achieve large frequency shifts with narrowband pulses. An all-fiber OPA was used to perform CARS imaging, but the longer pulse durations yield much lower peak powers than are available from solid-state sources [7]. Additionally, FWM tends to create noisy signal pulses [8]. This problem is alleviated in the fiber OPAs presented in [9,10] through the use of continuous-wave (CW) seeding. The source demonstrated in [9] is the only fiber source to provide comparable pulse parameters and energies to the

solid-state source [2]. OPOs that accomplish frequency conversion through FWM in PCF have been studied as well and are summarized in [11]. One designed for multimodal CARS imaging uses a femtosecond seed laser [12], resulting in low pulse energy (0.1–0.5 nJ) and low spectral resolution and efficiency.

Here we present a synchronously pumped fiber OPO based on the normal dispersion FWM process. The OPO achieves similar pulse parameters (2–4 ps duration and 3–4 nJ energy) to the OPA of [9], but with substantial performance and practical benefits over the OPA. For one, the self-consistent nature of the oscillator leads to significant reduction of the relative intensity noise (RIN) on the output pulse train. For another, the OPO reaches 13%–20% conversion efficiency to the signal wavelength, as compared to only 10% in the OPA. As a practical advantage, the OPO eliminates the CW seed laser used in [9,10]. The capabilities of this system are illustrated by its use in CARS imaging of mouse tissues.

Numerical simulations were used to guide the design of the OPO. The OPO is simulated with a generalized nonlinear Schrodinger equation that includes higher-order dispersion, spontaneous and stimulated Raman scattering (SRS), self-steepening, and input shot noise [13,14]. Each round trip, shot noise and pump pulses at 1035 nm, with 7.5 ps duration and 1.95 kW peak power, are injected into 31 cm of endlessly single-mode PCF with a zero-dispersion wavelength of 1051 nm. The dispersion coefficients at this wavelength are 1.59 fs^2/mm, 59.4 fs^3/mm, –69.3 fs^4/mm, 136 fs^5/mm, and –182 fs^6/mm, and the nonlinear parameter $\gamma = 9.6$ (W · km)$^{-1}$. We will refer to the short-wavelength photon as the signal and the long-wavelength photon as the idler. A 1300 nm long-pass filter is applied to the idler field to provide feedback, with a 5% feedback ratio chosen to account for coupling and other losses. A delay is applied to the idler pulse to synchronize the idler and pump pulses. Under these conditions, the fluctuations on the signal and idler fields prohibit stable operation of the OPO [Fig. 1(a)].
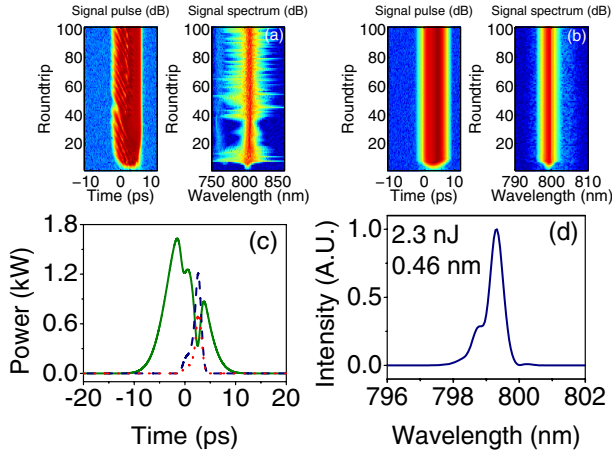
Fig. 1. Results of simulations. (a) Signal pulse and spectrum without filter. (b) Signal pulse and spectrum with filter. (c) Filtered FWM: pump (solid curve), signal (dashed curve), and idler (dotted curve) pulses. (d) Signal spectrum. The input pulse is centered at 1035 nm with 7.5 ps duration and 1.95 kW peak power. Idler feedback is centered at 1468 nm with a 2 nm Gaussian filter.

We propose that filtering the field fed back into the PCF will result in stable, narrow-band operation. Simulations indicate that stable signal pulses are generated for filter bandwidths around 2–3 nm. Figure 1(b) shows the resulting signal with the use of a 2 nm Gaussian filter. The filter effectively stabilizes the field that is fed back, which in turn stabilizes the signal and idler in the oscillator. Nearly transform-limited 1.4 ps pulses with 2.3 nJ energy [Figs. 1(c) and 1(d)] are generated at the signal frequency under these conditions. Thus the narrow filter is a critical element of the design.

The experimental setup is depicted in Fig. 2. A Yb-doped fiber laser (a modified PicoFYb from Toptica Photonics), tunable from 1031 to 1038 nm, is used to seed a divided-pulse amplifier (DPA) with 10 μm core fiber [15]. The output of the amplifier consists of 6.5–9 ps pulses with up to 2.5 W of average power at a repetition rate of 46 MHz. These pulses are coupled into a PCF with dispersion parameters matching those of the simulation and converted into signal and idler pulses. The signal light is coupled out of the OPO with a dichroic mirror, and a Gaussian filter with 2.7 nm bandwidth is created by a diffraction grating and fiber collimator, with the
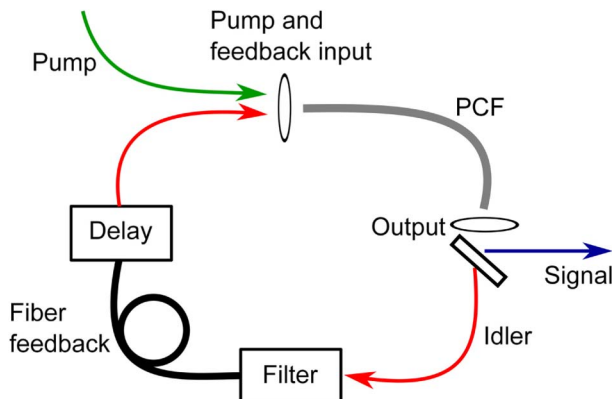
bandwidth chosen based on available gratings. Around 3.7 m of step-index fiber (Corning SMF28e+) forms the feedback loop, and a fiber-coupled delay line with up to 80 ps of delay allows synchronization. The feedback ratio is estimated to be around 2%. A half-wave plate matches the polarization of the field that is fed back to that of the pump. Around 300 mW of the amplifier output is picked off before the OPO for combination with the signal at the microscope. The free-space components used in this initial demonstration could be replaced by fiber-format components in the future.

Experimental results obtained with 31 cm of PCF are shown in Fig. 3. Pump pulses with 0.2 nm bandwidth and 8.7 ps duration are used [Figs. 3(a) and 3(b)]. With 850 mW (22 nJ) coupled into the PCF, 140 mW (3 nJ) is generated at the signal wavelength of 801 nm with a bandwidth of 0.5 nm and a duration of 2.1 ps, in good agreement with simulations. Higher pump powers yield signal powers up to around 200 mW (4.3 nJ), with slightly longer pulses, but the fluctuations increase; this will be discussed further below. Simulations indicate that longer PCFs generate higher pulse energies with more structured spectra due to coherent interactions between the pump and FWM fields as the process saturates. This is evidenced in the shoulder on the signal spectrum. The frequency difference between the pump and signal is 2850 cm^{-1}, which corresponds to the CH$_2$ stretching vibrational mode. The frequency shift can be tuned from 2740 to 3150 cm^{-1}, limited by the tuning range of the seed laser, with similar performance. The signal wavelength may be tuned over 2–3 nm by adjusting the center wavelength of the filter, and tuning over the broader range is accomplished by tuning the seed oscillator. Minimal realignment of the grating filter and delay line is required.

This OPO matches the pulse parameters of the solid-state device [2] and offers major performance advantages over other fiber-based sources. The peak signal power is twice that, and the average power three times that, of the fiber OPA reported in [10]. The peak power is 15 times that of the fiber source presented in [5], while the average power is eight times higher.
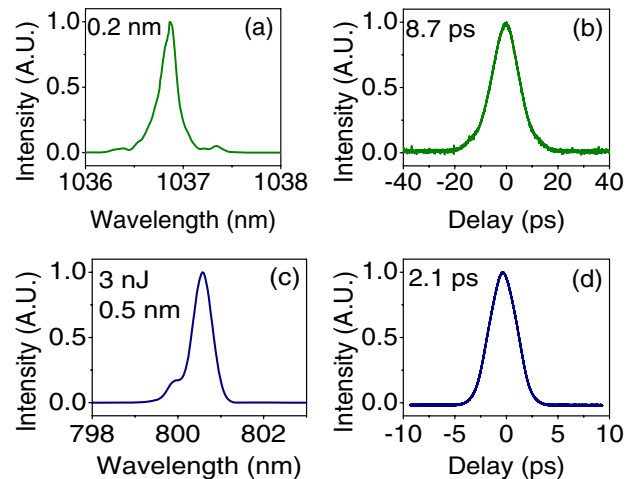

Fig. 2. Schematic experimental setup.

Fig. 3. Experimental results: picked-off pump (a) spectrum and (b) autocorrelation. Signal (c) spectrum and (d) autocorrelation with a 2850 cm^{-1} frequency shift from the pump.

The signal pulses are combined with the picked-off pump pulses and directed to an Olympus FV300 microscope with an Olympus XL Plan N 25X water-immersion objective with an NA of 1.05. We use epi-detected CARS with an estimated 80 mW of light delivered to the sample. CARS images at the 2850 cm^{-1} vibrational shift are presented in Fig. 4. Figures 4(a) and 4(b) show white matter and the cortex in a mouse brain section, respectively. Figure 4(c) shows the stratum corneum, and 4(d) shows a sebaceous gland around 36 µm deep in the mouse ear. The signal-to-noise ratio of the lipid droplets in the sebaceous gland images ranges from 150 to 200, and the signal-to-noise ratio for the myelin sheathes is around 60. Images were taken at 2–4 µs per pixel without averaging. The OPO provides both improved image quality and imaging speed over the fiber source presented in [9]. Imaging was also performed at the 2930 cm^{-1} vibrational resonance (Fig. 5) as an initial demonstration of the tunability of the OPO.

Compared to CARS, SRS microscopy has the advantages of being background-free and providing quantitative information on chemical concentration [16]. However, an extremely quiet source of pulses is required to detect SRS with an adequate signal-to-noise ratio for imaging. A fiber source that is quiet enough to perform SRS microscopy with direct detection has not been reported. Recent work has focused on alternate detection techniques that permit the use of fiber sources for SRS imaging, such as the collinear balanced detection described in [17] and the demonstrated use of CW diode lasers with dual modulation in [18]. However, these techniques come at the cost of added electronic complexity, and, in the case of the CW source, significantly lower SRS signal and imaging speed than can be achieved with a pulsed source.

SRS imaging is typically performed by modulating one of the pulse trains at around 10 MHz and detecting the
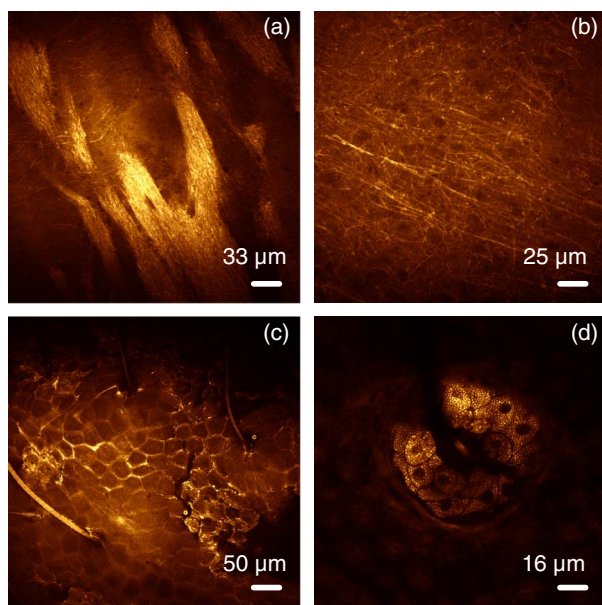

Fig. 5.   Epi-CARS images of sebaceous glands in mouse ear at the (a) 2850 cm^{-1} and (b) 2930 cm^{-1} frequency shifts, which show the increase in the protein signal at the 2930 cm^{-1} shift. 512×512 pixels at 2 µs per pixel, no averaging.

change in energy of the other pulse synchronously. RIN spectra for the source described here are shown in Fig. 6 along with that of the OPA based on the same FWM process [9]. The RIN of the seed laser is near the instrument floor of −165 dBc/Hz. After amplification, the RIN is around −155 dBc/Hz, and the OPO itself contributes 15 dBc/Hz across the spectrum in routine operation. The RIN of the fiber OPO is at least 20 dBc/Hz below that of the analogous OPA, which confirms the rationale for developing the OPO. However, the OPO is noisier than the target of −150 dBc/Hz for SRS imaging with direct detection.

The instruments described in [7] and [5] offer the practical benefits of all-fiber construction. Although the OPO described here relies on bulk optics for coupling and filtering, it should be possible to achieve similar performance in a fiber-integrated version. Fiber-format filters exist, and it is possible to splice step-index fibers to small-core PCF. A fiber-format filter would eliminate the need for minor realignment of the present system when the wavelength is tuned, which arises from the coupling of wavelength to path length in the grating-based filter. Future work will also explore noise reduction by creation of a lower-noise pump and through the design of the OPO. Additionally, the tuning range of the OPO could be expanded through the use of a different or more widely tunable pump laser or by using a PCF with a different dispersion profile.

Fig. 4.   Epi-CARS images at 2850 cm^{-1}. (a) White matter in mouse brain section. (b) Cortex in mouse brain section. (c) Stratum corneum. (d) Sebaceous gland in mouse ear. 512×512 pixels at 2–4 µs per pixel, no averaging.
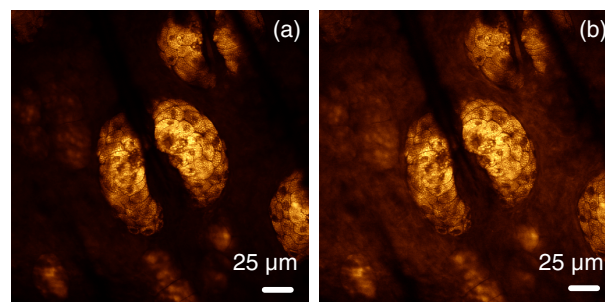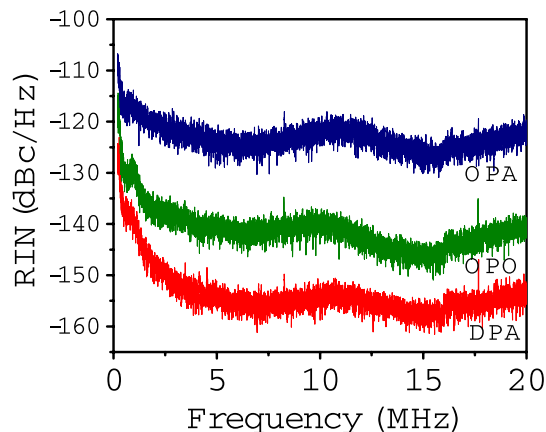

Fig. 6.   Megahertz RIN measurement on fiber sources for coherent Raman microscopy taken with a resolution bandwidth of 6.5 kHz. The OPA measurement references the work done in [9].

In conclusion, we have demonstrated a picosecond fiber OPO based on FWM in PCF. The use of a narrowband filter in the feedback loop is critical for stable operation of the OPO. The OPO matches the pulse parameters of solid-state sources and a fiber OPA, with intensity fluctuations much lower than the fiber OPA but greater than the solid-state OPO. Among fiber sources, the performance is the best reported to date and yields CARS images with excellent signal-to-noise performance and fast imaging speeds.

References

1. C. L. Evans and X. S. Xie, Annu. Rev. Anal. Chem. **1**, 883 (2008).
2. F. Ganikhanov, S. Carrasco, X. S. Xie, M. Katz, W. Seitz, and D. Kopf, Opt. Lett. **31**, 1292 (2006).
3. K. Kieu, B. G. Saar, G. R. Holtom, X. S. Xie, and F. W. Wise, Opt. Lett. **34**, 2051 (2009).
4. G. Krauss, T. Hanke, A. Sell, D. Träutlein, A. Leitenstorfer, R. Selm, M. Winterhalder, and A. Zumbusch, Opt. Lett. **34**, 2847 (2009).
5. K. Kieu and N. Peyghambarian, Proc. SPIE **7903**, 790310 (2011).
6. E. R. Andresen, C. K. Nielsen, J. Thøgersen, and S. R. Keiding, Opt. Express **15**, 4848 (2007).
7. M. Baumgartl, T. Gottschall, J. Abreu-Afonso, A. Dez, T. Meyer, B. Dietzek, M. Rothhardt, J. Popp, J. Limpert, and A. Tünnermann, Opt. Express **20**, 21010 (2012).
8. P. J. Mosley, S. A. Bateman, L. Lavoute, and W. J. Wadsworth, Opt. Express **19**, 25337 (2011).
9. S. Lefrancois, D. Fu, G. R. Holtom, L. Kong, W. J. Wadsworth, P. Schneider, R. Herda, A. Zach, X. S. Xie, and F. W. Wise, Opt. Lett. **37**, 1652 (2012).
10. M. Chemnitz, M. Baumgartl, T. Meyer, C. Jauregui, B. Dietzek, J. Popp, J. Limpert, and A. Tünnermann, Opt. Express **20**, 26583 (2012).
11. J. E. Sharping, J. Lightwave Technol. **26**, 2184 (2008).
12. Y.-H. Zhai, C. Goulart, J. E. Sharping, H. Wei, S. Chen, W. Tong, M. N. Slipchenko, D. Zhang, and J.-X. Cheng, Appl. Phys. Lett. **98**, 191106 (2011).
13. J. Hult, J. Lightwave Technol. **25**, 3770 (2007).
14. R. Paschotta, Opt. Express **18**, 5041 (2010).
15. S. Zhou, F. W. Wise, and D. G. Ouzounov, Opt. Lett. **32**, 871 (2007).
16. C. W. Freudiger, W. Min, B. G. Saar, S. Lu, G. R. Holtom, C. He, J. C. Tsai, J. X. Kang, and X. S. Xie, Science **322**, 1857 (2008).
17. K. Nose, Y. Ozeki, T. Kishi, K. Sumimura, N. Nishizawa, K. Fukui, Y. Kanematsu, and K. Itoh, Opt. Express **20**, 13958 (2012).
18. C.-R. Hu, M. N. Slipchenko, P. Wang, P. Wang, J. D. Lin, G. Simpson, B. Hu, and J.-X. Cheng, Opt. Lett. **38**, 1479 (2013).